Synchronization Parameters and Perfusion Improvement after Cardiac Resynchronization Therapy

A Peix, I González, R Zayas, L Rodríguez, M Quiñones, J Valiente, L Cabrera, Y Fayad, N de Armas

Citation

A Peix, I González, R Zayas, L Rodríguez, M Quiñones, J Valiente, L Cabrera, Y Fayad, N de Armas. *Synchronization Parameters and Perfusion Improvement after Cardiac Resynchronization Therapy*. The Internet Journal of Cardiology. 2007 Volume 6 Number 1.

Abstract

To evaluate the modification of hemodynamic parameters and of synchrony using radionuclide angiography (RNA), as well as the effect on myocardial perfusion, 20 patients with dilated cardiomyopathy (DCM) were studied before and five months after cardiac resynchronization therapy (CRT),. Inter- and intraventricular synchronization was assessed by phase analysis. After CRT, left ventricular ejection fraction improved from 22 ± 5% to 29 ± 13%, p=0.04. There was a significant reduction of intraventricular asynchrony in ischemic patients. There was no difference between inter- and intraventricular asynchrony measured by RNA and echocardiography at baseline nor for the improvement after CRT. The summed rest score (SRS) decreased from 33±14 to 21±12 (p=0.004). SRS reduced from 35±12 to 27±9 (p NS) among ischemic patients, and from 31±17 to 17±11 (p=0.02) among non-ischemic. Radionuclide angiography is a useful method to assess heart failure patients before and after CRT. CRT improves myocardial perfusion mainly in non-ischemic patients.

INTRODUCTION

Cardiac resynchronization therapy (CRT) has shown hemodynamic [1,2,3] and clinical [2,3,4,5] improvement, as well as a reduction of electrical asynchrony [6,7,8] in patients with dilated cardiomyopathy (DCM) and intra- and/or interventricular asynchrony.

Although mostly echocardiography (and especially tissue Doppler imaging) is used to assess the degree of intra- and interventricular asynchrony [9], other noninvasive techniques such as radionuclide angiography (RNA) and magnetic resonance tagging provide indirect information about cardiac conduction pathways through contractility parameters.

RNA allows not only global left ventricular function assessment with more reproducibility than echocardiography, but also the measurement of ventricular volumes and mitral regurgitation index. Furthermore, using phase analysis in RNA, a colour scale-coded image of the regional phase angles can be obtained as a map of sequential contraction, which is related to the depolarization wave. Therefore, cardiac conduction and synchronization parameters can also be evaluated by RNA [6,7,10].

Ischemic heart disease and old age have been found to be significant predictors of a poor response to CRT [11]. Duncan et al demonstrated that patients with idiopathic DCM show significantly more extensive left ventricle (LV) remodelling than do those with ischemic DCM [3], and Sciagrà et al found that, despite clinical improvement, patients with severe resting perfusion defects do not show significant improvement in left ventricular ejection fraction (LVEF) or reduction in LV volumes [12]. The effect of CRT on oxygen consumption and myocardial blood flow has also been studied by PET [13,14], but the combination of data of function, synchronism and perfusion given by nuclear medicine studies could be a good approach for the evaluation of patients before and after CRT, an approach which has not been sufficiently exploited up to now.

Thus, the aim of this prospective study was to evaluate, by means of RNA, the modification of both hemodynamic parameters and synchrony due to CRT, comparing synchrony with echocardiographic data. A second aim was also to evaluate the effect of CRT on myocardial perfusion assessed by SPECT scintigraphy.

METHODS

STUDY POPULATION

Twenty consecutive patients (14 men and 6 women, mean age: 56 ± 11 years) with refractory heart failure (New York Heart Association –NYHA- class III or IV), depressed LVEF (<35%), QRS width >120 ms, and substantial LV dyssynchrony were prospectively included for implantation of a CRT device. Eight of them (40%) had an ischemic DCM (five with a previous myocardial infarction), while the others were idiopathic. Etiology was considered ischemic in the presence of significant coronary artery disease (50% stenosis in one or more of the major epicardial coronary arteries) or a history of myocardial infarction.

The study design was approved by the Review Board of the Institute of Cardiology, and a written informed consent to participate was obtained from all patients before CRT. Patients were studied before (baseline) and on an average of 5.2 months after pacemaker implantation.

The clinical evaluation was performed by an independent cardiologist blinded to all other data. The functional evaluation included a NYHA class and six-minute walking distance [15]. In all cases, QRS duration was measured from the surface electrocardiogram (ECG) using the widest QRS complex from the leads DII, V1, and V6.

RADIONUCLIDE ANGIOGRAPHY

Radionuclide angiography was performed using the in vivo method of red blood cells labelling (2 ml Na-pyrophosphate IV; 400 mg K^+ perchlorate per os; 740 MBq of ^{99m} Tc IV). A gated blood-pool equilibrium RNA was acquired in the left anterior oblique projection, with an incidence between 30° and 60° (best septal visualization) and a 10° to 15° caudal tilt, with the patient lying supine. A single-head gamma camera (Siemens Orbiter), equipped with a low energy, all-purpose collimator was used. Twenty-four 64 x 64 ECG-gated frames per cardiac cycle were acquired with 10 x 10^6 counts, and a 10% rejection window was set around the average R-R interval. Images were normalized and filtered for space-time high-frequency noise.

Variable left ventricular regions of interest (ROI) were constructed with a semiautomatic edge detection algorithm in each time frame. Scintigrams were encoded for amplitude, setting background pixels below 25% of maximal amplitude to zero, which provided clearer ventricular edges for ROI detection [8]. After background subtraction, LVEF was calculated from the corresponding activity-time curves as: EF = (end diastolic counts – end systolic counts) / (end diastolic counts - background counts). LVEF >50% was considered normal.

The LV peak filling rate was determined from the activity-time curve as the maximum positive of dV/dt and expressed as end-diastolic volume per second (EDV/s).

For assessment of mitral regurgitation, a two-factor analysis was applied (ventricles and atria plus great vessels) using the DiPaola algorithm [16] after which the regurgitation index (RI) was obtained with the following formula: RI = Left SV counts / Right SV counts [17,18]. Values of 1.3 ± 0.8 were considered normal [17].

Phase analysis was performed using a software which performs an independent Fourier assessment [6,10] based on the fact that within the ventricular region, the phase angle of each pixel is proportional to the time of maximal activity change. A colour-coded image of the end-systolic phase angle is generated as a map of sequential contraction after computation of the Fourier transform. ROIs were constructed over LV, RV, LV septum (S), lateral (L), anterior (ANT) and inferior (INF) walls, as well as over base (B) and apex (A).

Interventricular activation time (T_{RV-LV}) was calculated from the difference between RV and LV phase peaks of the phase histogram, with a mean time resolution of ± 5ms [6]. Intraventricular activation duration was computed from the distribution of phase angles within the LV ROI (T_{S-LW} and $T_{ANT-INF}$). LV and RV contraction onset (T_{0-LV} and T_{0-RV}), as well as S, L, ANT, INF, B and A contraction onset (T_{0-S}, T_{0-L}, T_{0-ANT},

T_{0-INF}, T_{0-B}, T_{0-A}) were also measured. Published normal values in milliseconds (ms) are: T_{RV-LV} = 2 ± 25 ms; T_{S-LW} = 4 ± 22 ms [10]; Apex to base delay (T_{A-B}): 2 ± 16 ms [6].

MYOCARDIAL SCINTIGRAPHY

A SPECT ^{99m} Tc-MIBI scintigraphy was performed at rest before (baseline), and three months after pacemaker implantation. Images were acquired 45 minutes to one hour after the intravenous injection of 740 MBq of ^{99m} Tc-MIBI, with a rotating dual-head gamma camera (Sopha SMV) equipped with a low-energy, high-resolution parallel-hole collimator centered on the 140 keV photopeak with a 20% window. Thirty-two projections (25 seconds per projection), with a 64x64 matrix were obtained over an 180 orbit. Filtered back-projection was then made with a low-resolution Butterworth filter with a cutoff frequency of 0.25

cycles per pixel, order 7. No attenuation or scatter correction was applied.

SCINTIGRAPHIC IMAGE INTERPRETATION

The semiquantitative visual interpretation of images employed short-axis and vertical long-axis tomograms divided into 17 segments for each patient [19]. Each segment was scored by the consensus of two expert independent observers who were unaware of the clinical and angiographic data, using a five-point scoring system (from 0 = normal to 4 = absence of myocardial uptake). Disagreements in image interpretation, including every score in each SPECT segment, were resolved by consensus.

ECHOCARDIOGRAPHY

Echocardiographic analysis was done with high-resolution ultrasound equipment (Philips iE33 2006, version 2.0.1.420) with a S25-1 transducer (from 1.3 to 3.6 MHz). For Doppler Tisular Imaging (DTI), color Doppler frame rates varied between 150 and 400 frames/s depending on the sector width of the range of interest and aliasing velocities between 16 and 32cm/s. The digital cineloops were analyzed using commercial software (Philips) by offline analysis. The sample volume was placed in basal portions of the septum, lateral, inferior, and anterior walls (using the apical four-, and two-chamber images) to derive velocity profiles. Myocardial velocity curves were obtained, and regional systolic velocity (Sm) during ejection phase, early diastolic velocity (Em), as well as the time to peak Sm (Ts) and time to peak Em (Te) were measured. For the measurement of timing, the beginning of the QRS complex was used as the reference point. To assess LV synchronicity, SD of Ts (Ts-SD) and Te (Te-SD) of all the 12 segments were computed. The higher the values, the more severe the LV asynchrony. The cut-off value for asynchrony septum-lateral was 65 ms.

CRT IMPLANTATION

A coronary sinus venogram was obtained using a balloon catheter, followed by the insertion of the LV pacing lead. An 8F guiding catheter was used to position the LV lead in the coronary sinus, preferably in the lateral or postero-lateral vein. The right atrial and ventricular leads were positioned conventionally. All leads were connected to a dual chamber ventricular ICD.

STATISTICAL ANALYSIS

For reasons of uniformity and the reduced number of patients studied, summary statistics for continuous variables obtained from the radionuclide angiography are presented as medians. The other continuous variables were expressed as mean ± 1 standard deviation. Each patient was his or her own control at follow-up. Continuous variables were analyzed using the Wilcoxon matched-pair test between baseline and follow-up, and data from ischemic and non-ischemic patients were analyzed by the Mann-Whitney U test. For comparison of asynchrony data obtained by RNA and echocardiography the McNemar test was used. A p value < 0.05 was considered significant.

RESULTS

Patients' characteristics and clinical improvement after CRT

Implantation was successful and without complications in all patients. Due to potentially lethal ventricular arrhythmias, in eight patients (40%) the automatic implantable defibrillation function was also activated.

At baseline, 11 patients (55%) had a NYHA functional class III, and the other nine, a class IV. After a mean of 5.2 months of CRT, four patients improved by one NYHA functional class and 14 patients improved by two. No patients stayed in class IV. Ischemic patients improved more than non-ischemic: 88% achieved a NYHA class I, and only one showed a class II. On the contrary, among the non-ischemic patients, 54% attained a class II and one stayed in class III. Thirty-three percent of patients showed a six-minute walking distance ? 300 m at baseline, which in all cases increased after CRT.

Two patients (non-ischemic) died of worsening heart failure before the three-month follow-up evaluation. One patient (of ischemic etiology) died after the evaluation due to an infectious endocarditis on the pacemaker electrodes.At follow-up, QRS width decreased from 171 ± 34 ms to 116 ± 25 ms, and the PR interval also decreased from 179 ± 34 ms to 110 ± 24 ms ($p=0.0001$ in both cases).The mean LVEF at baseline was 22%.

VENTRICULAR FUNCTION

After CRT, there was a significant LVEF improvement (from 22±5% to 30±13%, $p=0.04$). Diastolic function improved, but not significantly: from 1.39±0.83 to 1.89±0.93 End-Diastolic Volume / second (EDV/s). The regurgitation index showed an important reduction after CRT (from 2.2±0.7 to 1.8±0.5, $p<0.03$). No significant difference was observed in the ventricular functional improvement according to the etiology of the DCM.

SYNCHRONIZATION PARAMETERS

Mean $T_{0\text{-}LV}$ and $T_{0\text{-}RV}$ decreased from 111 ms to 105 ms and from 67 ms to 59 ms (p NS), respectively.Regarding interventricular synchronism, mean $T_{RV\text{-}LV}$ reduced from 76 to 54 ms, although it was non significant. Mean intraventricular asynchronism ($T_{S\text{-}LW}$ and $T_{ANT\text{-}INF}$) reduced from 137 to 70 ms and from 67 to 49 ms, respectively. The onset of contraction in the different walls is shown in Figure 1. All walls except the apex and inferior wall started contraction earlier after CRT. In the case of apex – base contraction, CRT reversed the apex-to-base ventricular activation sequence, causing early contraction of the LV base followed by the apex.

Figure 1

Figure 1: Times of onset of contraction in the different walls. White bars represent baseline values and the black ones correspond to the values three months after CRT.

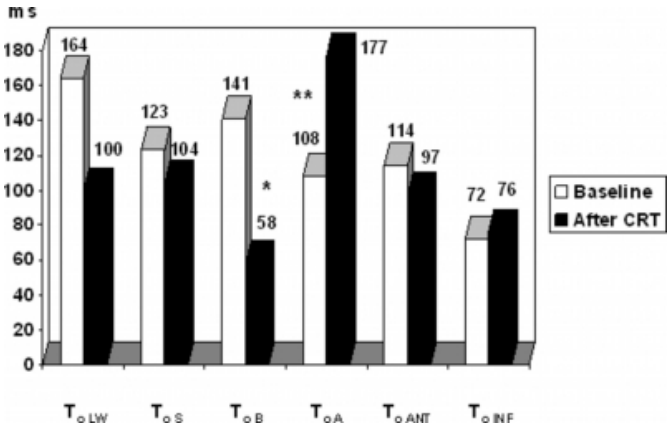

* p = 0.0009 ** p = 0.01

$T_{0\,S}$: septal contraction onset; $T_{0\,LW}$: lateral wall contraction onset; $T_{0\,B}$: basal contraction onset; $T_{0\,A}$: apex contraction onset; $T_{0\,ANT}$: anterior contraction onset; $T_{0\,INF}$: inferior contraction onset; CRT: cardiac resynchronyzation therapy

Inferior-to-anterior wall ventricular activation sequence was always in the right direction, but with a bigger delay at baseline, which reduced after CRT.

Figure 2 shows the evolution of ventricular asynchrony after CRT according to the etiology of the heart disease. Only in ischemic patients, the reduction of intraventricular dyssynchrony measured by the $T_{S\text{-}LW}$ was significant (p=0.02). Regarding the intraventricular dyssynchrony measured by the $T_{ANT\text{-}INF}$, again the ischemic patients were those who experienced the biggest reduction, although non significant.

Figure 2

Figure 2: Intraventricular synchronism (septal-lateral wall and anterior-inferior). Comparison between ischemic and non-ischemic patients. White bars represent baseline values and the black ones correspond to the values three months after CRT.

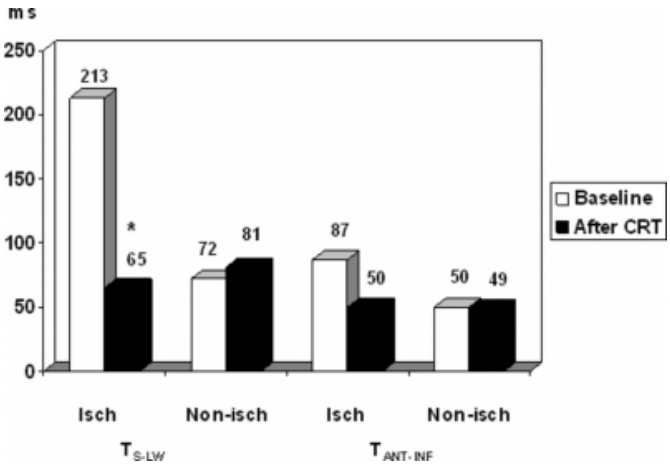

* p = 0.01

$T_{S\text{-}LW}$: septal – lateral wall contraction time; $T_{ANT\text{-}INF}$: anterior – inferior contraction time; CRT: cardiac resynchronization therapy

RADIONUCLIDE ANGIOGRAPHY VS. ECHOCARDIOGRAPHY

There was no difference between inter- and intraventricular dyssynchrony measured by RNA and echocardiography at baseline, nor for the improvement after CRT (see Tables 1 and 2).

Figure 3

Table 1: Interventricular Dyssynchrony. Radionuclide angiography vs. Echocardiography

A) At Baseline

		Dyssynchrony by Echocardiography	
		YES	NO
Dyssynchrony by RNA	YES	16	1
	NO	1	0

A) Improvement Post CRT

		By Echocardiography	
		YES	NO
By RNA	YES	15	0
	NO	2	1

CRT: cardiac resynchronization therapy; RNA: radionuclide angiography

In both cases, p NS

Figure 4

Table 2: Intraventricular Dyssynchrony. Radionuclide angiography vs. Echocardiography

A) At Baseline

		Dyssynchrony by Echocardiography	
		YES	NO
Dyssynchrony by RNA	YES	16	1
	NO	0	1

A) Improvement Post CRT

		By Echocardiography	
		YES	NO
By RNA	YES	12	2
	NO	4	0

CRT: cardiac resynchronization therapy; RNA: radionuclide angiography

In both cases, p NS

MYOCARDIAL PERFUSION

Mean baseline summed rest score (SRS) was 33±14 and the mean number of affected segments per patient was 3. In the whole group of patients, myocardial perfusion significantly improved after CRT: the SRS decreased from 33±14 to 21±12 (p=0.004) and the mean number of affected segments was 2.

SRS reduced from 35±12 to 27±9 (p NS) among ischemic patients, and from 31±17 to 17±11 (p=0.02) among non-ischemic patients.

DISCUSSION

Phase analysis of gated cardiac blood pool is a useful and accepted method for the localization of the contraction (pacemaker) onset and the measurement of the magnitude and characterization of the sequence of regional contraction which reflects electrical conduction [20]. Compared with echocardiography, the technique is independent of the acoustic window and more reproducible. Furthermore, RNA can be applied in the presence of pacemakers, unlike nuclear magnetic resonance cardiac imaging and, as our results prove, constitutes a comparable method with echocardiography to assess the synchronization times both

for deciding whether to implant the biventricular pacing and for follow-up.

Kerwin et al [8] found that changes in LVEF with pacing exceeded the measured interobserver variability, suggesting that interventricular dyssynchrony was a correctable parameter contributing to LV dysfunction. In our cases the T_{RV-LV}, as a manifestation of interventricular dyssynchrony, reduced at five months after CRT, but the reduction was not significant, probably due to the small sample included.

Among our cases, the intraventricular dyssynchrony was present mainly between septal and lateral walls. But it was only in ischemic patients where the reduction of intraventricular dyssynchrony after CRT, measured by the T_{S-LW}, was significant. Inferior-to-anterior wall ventricular activation sequence was always in the right direction, but with a bigger delay at baseline, which reduced after CRT, and again the ischemic patients were those who experienced the biggest reduction, although non significant. We have not found any reference stating differences between synchronization times according to the etiology of the heart failure. Ours were not impressive and, evidently, more patients and further investigation are necessary. Nonetheless, this difference could account for the bigger improvement in clinical status among ischemic patients, taking into account that effective pumping by both ventricles requires this synchronous type of contraction.

Decreased diastolic time is one of the proposed mechanisms to explain cardiac abnormalities found in isolated LBBB [21]. Patients in our study showed a moderate peak filling rate reduction at baseline, which improved at follow-up after a mean of five months of CRT, becoming a minor abnormality.

Functional mitral regurgitation in DCM results from an imbalance between the closing and the tethering forces that act on the mitral valve leaflets [22]. Ventricular dilation and chamber sphericity increase the distance between the papillary muscles and the enlarged mitral annulus, restricting leaflet motion and increasing the force needed for effective mitral valve closure [22,23,24]. Breithardt et al [25] found that LV systolic function improvement after CRT causes an accelerated rise in the transmitral pressure gradient, which effectively counteracts the increased tethering forces that impair mitral valve competence. We considered that the reduction of the regurgitation index, as has been found before in heart failure patients after certain treatments (for example, postcardiomyoplasty) [18], has been the main factor contributing to the functional improvement in our cases. Also, the reverse remodelling process that occurs chronically in these patients, which was present in 35% of our patients, contributes to a further decrease in functional mitral regurgitation severity [14,26]. This small number could be related to the fact that our patients had only a three-month follow-up, while in other studies the reverse remodelling has been evaluated at a longer interval of time (six months or more after CRT) [14,26].

Although the overall time necessary to activate all ventricular regions is not changed by the CRT, its regional effect on the septum, through less ventricular asynchrony [7], and its restitution of a coordinated base-apex activation [7], as we can see in this study, may also explain the systolic function improvement, mainly in the left ventricle. We did not find significant differences in systolic function improvement according to the etiology of the heart failure, as observed by other authors [27,28].

Echocardiography is mostly used nowadays to assess the intra- and interventricular dyssynchrony before and after CRT, providing useful and practical selection criteria for this therapy. However, it is important to point out that RNA is more reproducible, and offers comparable data. Besides, considering the new possibilities given by phase analysis using gated SPECT [29], which allows for the analysis of both functional and perfusion data with the same study, nuclear medicine techniques should be taken into account for assessment of patients before and after CRT.

It is important to point out that LBBB causes septal hypoperfusion and hypokinesia. Vernooy et al [30], in an experimental study, suggested that this septal hypoperfusion appears to be primarily determined by reduced septal workload. On the other hand, septal glucose metabolism is also reduced and seems to be improved by CRT without significant changes [31] or with only a mild influence on myocardial perfusion [37]. According to Neri [31], CRT not only improves myocardial wall function but could also induce normalization of the myocardial metabolism in the septum, suggesting a better use of glucose as a metabolic substrate without interfering with cellular membrane pumps observed in LBBB [33]. Therefore, resynchronisation of the septum contraction does require this increased energy consumption.

It has been suggested that CRT rebalances the loading conditions of the heart [13]. Knaapen et al have found that resting myocardial blood flow (MBF) is unaltered by CRT

despite an increase in LV function; however, the distribution pattern of resting MBF becomes more homogeneous [13]. There are two explanations for the improved myocardial perfusion. First, congestive heart failure is accompanied by increased LV filling pressure and wall stress, both of which may affect myocardial perfusion through extravascular compression of the coronary vascular bed [34], and which are reduced by CRT [35,36]. Second, myocardial perfusion is predominantly a diastolic process, and dyssynchrony of the heart reduces diastole by shortening the LV filling time [37], which can be increased by CRT. In general, we found a significant reduction of the SRS after CRT, but this difference was more important in non-ischemic patients: from 31±17 to 17±11 (p=0.02), compared with the ischemic, where the SRS only reduced from 35±12 to 27±9 (p NS). These results coincide with those of other studies [13,14]. Flow-limited stenoses and the presence of scar tissue in five cases may be responsible for these differences.

Recently, it has been demonstrated by using SPECT imaging with technetium-99m tetrofosmin [38] and by using 18F-FDG SPECT [39], that the extension of scar tissue and viable myocardium are directly related to the response to CRT, and that scar tissue in the LV pacing lead region may prohibit response to CRT. We did not perform viability studies in this group of patients, but the site of lead implantation was the posterolateral wall, where there was no infarction among our cases.

LIMITATIONS OF THE STUDY

1. A small number of patients were included.
2. Gated blood-pool SPECT was not used. Thus, the factor analysis was applied (as an alternative approach) to separate overlapping structures, in order to assess the regurgitation index.
3. A myocardial viability analysis was not performed before CRT implantation.

CONCLUSIONS

Radionuclide angiography is a useful method to assess heart failure patients before and after CRT. CRT improves myocardial perfusion mainly in non-ischemic patients.

ACKNOWLEDGMENT

We are grateful to Adrienne Hunter, Ph.D, for her patience and dedication in reviewing the manuscript.

CORRESPONDENCE TO

Amalia Peix, MD, PhD Nuclear Medicine Department Institute of Cardiology 17 No. 702, Vedado. CP 10 400 La Habana. Cuba Phone: (537) 830 6139 Fax: (537) 834 Email: peix@infomed.sld.cu

References

1. Blanc JJ, Etienne Y, Gilard M, et al. Evaluation of different ventricular pacing sites in patients with severe chronic heart failure: results of an acute hemodynamic study. Circulation 1997;96:3273-7
2. Leclercq C, Cazeau S, Victor F, Lazarus A, Daubert JC. Long-term results of permanent ventricular pacing in patients with refractory heart failure. Eur Heart J 1998;19:573-9
3. Duncan A, Wait D, Gibson D, Daubert JC. Left ventricular remodelling and haemodynamic effects of multisite biventricular pacing in patients with left ventricular systolic dysfunction and activation disturbances in sinus rhythm: sub-study of the MUSTIC trial. Eur Heart J 2003;24:430-41
4. Gras D, Mabo P, Tang T, et al. Multisite pacing as a supplemental treatment of chronic heart failure: preliminary results of the Medtronic Inc. Insync study. Pacing Clin Electrophysiol 1998;21:2249-55
5. Abraham WT, Fisher WG, Smith AL, et al. Cardiac resynchronization in chronic heart failure. N Engl J Med 2002;346:1845-53
6. Toussaint JF, Peix A, Lavergne T, et al. Reproducibility of the ventricular synchronization parameters assessed by multiharmonic phase analysis of radionuclide angiography in the normal heart. Int J Cardiovasc Imaging. 2002;18:187-94
7. Toussaint JF, Lavergne T, Ollitraut J, et al. Biventricular pacing in severe heart failure patients reverses electromechanical dyssynchronization from apex to base. Pacing Clin Electrophysiol 2000;23:1731-6
8. Kerwin WF, Botvinick EH, O'Connell W, et al. Ventricular contraction abnormalities in dilated cardiomyopathy: effect of biventricular pacing to correct interventricular dyssynchrony. J Am Coll Cardiol 2000;35:1221-7
9. Bax JJ, Ansalone G, Breithardt OA, et al. Echocardiographic evaluation of cardiac resynchronization therapy: ready for routine clinical use?: A critical appraisal. J Am Coll Cardiol 2004;44:1-9
10. Peix A, Ponce F, Zayas R, et al. Evaluación de la sincronización ventricular por análisis de fase de Fourier en una ventriculografía radioisotópica. Rev Esp Med Nuclear 2003;22:26-30
11. Reuter S, Garrigue S, Bordachar P, et al. Intermediate-term results of biventricular pacing in heart failure: correlation between clinical and hemodynamic data. Pacing Clin Electrophysiol 2000;23:1713-7
12. Sciagrà R, Giaccardi M, Porciani MC, et al. Myocardial perfusion imaging using gated SPECT in heart failure patients undergoing cardiac resynchronization therapy. J Nucl Med 2004;45:164-8
13. Knaapen P, van Campen L, de Cock CC, et al. Effects of cardiac resynchronization therapy on myocardial perfusion reserve. Circulation 2004;110:646-51
14. Lindner O, Vogt J, Kammeir A, et al. Effect of cardiac resynchronization therapy on global and regional oxygen consumption and myocardial blood flow in patients with non-ischaemic and ischaemic cardiomyopathy. Eur Heart J 2005;26:70-6

15. Lipkin DP, Scriven AJ, Crake T, Poole-Wilson PA. Six minute walking test for assessing exercise capacity in chronic heart failure. Br Med J (Clin Res Ed) 1986;292:653-5
16. Cavaiolles F, Bazin JP, DiPaola R. Factor analysis in gated cardiac studies. J Nucl Med 1984;25:1067-71
17. Fránquiz JM, Cabrera C, Dorticós F, Maltas AM. Assessment of left ventricular function by equilibrium-gated angiography before and following latissimus dorsi cardiomyoplasty in dilated cardiomyopathy. Am J Noninvas Cardiol 1992;6:197-200
18. Peix A, Taín J, Cabrera C, et al. Radionuclide ventriculography in dynamic cardiomyoplasty. J Nucl Biol Med 1994;38:535-9
19. Cerqueira MD, Weissman MD, Dilsizian V, et al. Standardized myocardial segmentation and nomenclature for tomographic imaging of the heart. Circulation 2002; 105:539-42
20. Botvinick E, Frais M, Shosa D, et al. An accurate means of detecting and characterizing abnormal patterns of ventricular activation by phase image analysis. Am J Cardiol 1982;50:289-97
21. Grines CL, Bashore TM, Boudoulas H, Olson S, Shafer P, Wooley CF. Functional abnormalities in isolated left bundle branch block. The effect of interventricular asynchrony. Circulation 1989;79:845-53
22. Otsuji Y, Handschumacher MD, Schwammenthal E, Jiang L, Song JK, Guerrero JL. Insights from three-dimensional echocardiography into the mechanism of functional mitral regurgitation: direct in vivo demonstration of altered leaflet tethering geometry. Circulation 1997;96:1999-2008
23. Sabbah HN, Kono T, Rosman H, Jafri S, Stein PD, Goldstein S. Left ventricular shape: a factor in the etiology of functional mitral regurgitation in heart failure. Am Heart J 1992;123:961-6
24. Otsuji Y, Kumanohoso T, Yoshifuku S, et al. Isolated annular dilation does not usually cause important functional mitral regurgitation: comparison between patients with lone atrial fibrillation and those with idiopathic or ischemic cardiomyopathy. J Am Coll Cardiol 2002;39:1651-6
25. Breithardt O, Sinha AM, Schwammenthal E, et al. Acute effects of cardiac resynchronization therapy on functional mitral regurgitation in advanced systolic heart failure. J Am Coll Cardiol 2003;41:765-70
26. Jansen AH, Van Dantzig JM, Bracke F, et al. Qualitative observation of left ventricular multiphasic septal motion and septal-to-lateral apical shuffle predicts left ventricular reverse remodeling after cardiac resynchronization therapy. Am J Cardiol 2007;99:966-9
27. Molhoek SG, Bax JJ, van Erven L, et al. Comparison of benefits from cardiac resynchronization therapy in patients with ischemic cardiomyopathy versus idiopathic dilated cardiomyopathy. Am J Cardiol 2004;93:860-3
28. Waggoner AD, Rovner A, de las Fuentes L, et al. Clinical outcomes after cardiac resynchronization therapy: importance of left ventricular diastolic function and origin of heart failure. J Am Soc Echocardiogr 2006;19:307-13
29. Henneman MM, Chen J, Dibbets-Schneider P, et al. Can LV dyssynchrony as assessed with phase analysis on gated myocardial perfusion SPECT predict response to CRT? J Nucl Med 2007;48:1104-11
30. Vernooy K, Verbeek X, Peschar M, et al. Left bundle branch block induces ventricular remodelling and functional septal hypoperfusion. Eur Heart J 2005;26:91-8
31. Neri G, Zanco P, Zanon F, Buchberger R. Effect of biventricular pacing on metabolism and perfusion in patients affected by dilated cardiomyopathy and left bundle branch block: evaluation by positron emission tomography. Europace 2003;5:111-5
32. Nowak B, Sinha AN, Schaefer WM, et al. Cardiac resynchronization therapy homogenizes myocardial glucose metabolism and perfusion in dilated cardiomyopathy and left bundle branch block. J Am Coll Cardiol 2003;41:1523-8
33. Althoefer C. LBBB: challenging our concept of metabolic heart imaging with fluorine-18-FDG and PET? J Nucl Med 1998;39:263-5
34. Kjekshus JK. Mechanism for flow distribution in normal and ischemic myocardium during increased ventricular preload in the dog. Circ Res 1973;33:489-99
35. Leclerq C, Kass DA. Retiming the failing heart: principles and current clinical status of cardiac resynchronization. J Am Coll Cardiol 2002;39:194-201
36. Kass DA. Ventricular remodelling: chamber dyssynchrony and effects of cardiac resynchronization. Eur Heart J Suppl 2003;5:154-63
37. Zhou Q, Henein M, Coats A, Gibson D. Different effects of abnormal activation and myocardial disease on left ventricular ejection and filling times. Heart 2000;84:272-6
38. Ypenburg C, Schalij MJ, Bleeker GB, et al. Impact of viability and scar tissue on response to cardiac resynchronization therapy in ischaemic heart failure patients. Eur Heart J 2007;28:33-41
39. Ypenburg C, Schalij MJ, Bleeker GB, et al. Extent of viability to predict response to cardiac resynchronization therapy in ischemic heart failure patients. J Nucl Med 2006;47:1565-70

Author Information

Amalia Peix, MD, PhD
Nuclear Medicine Department, Institute of Cardiology

Iovank González, MD
Nuclear Medicine Department, Institute of Cardiology

Roberto Zayas, MD, PHD
Electrophysiology Department, Institute of Cardiology

Lydia Rodríguez, BSc
Biostatistics Department, Institute of Cardiology

Miguel Quiñones, MD
Electrophysiology Department, Institute of Cardiology

Juan Valiente, MD
Echocardiography Department, Institute of Cardiology

Lázaro O. Cabrera, MD
Nuclear Medicine Department, Institute of Cardiology

Yanela Fayad, MD
Electrophysiology Department, Institute of Cardiology

Nurys de Armas, MD
Biostatistics Department, Institute of Cardiology